DOI: 10.1002/ejic.200600887

Synthesis, Crystal Structures, and Photoluminescence of a Series of Coordination Polymers with Two Homologous Functional Flexible Ligands

Hong-Ping Zhou,*[a] Peng Wang,[a] Zhang-Jun Hu,[a] Lin Li,[a] Jing-Jin Chen,[a] Yang Cui,[a] Yu-Peng Tian,*[a–c] Jie-Ying Wu,[a] Jia-Xiang Yang,[a] Xu-Tang Tao,[b] and Min-Hua Jiang[b]

Keywords: Coordination polymers / Flexible ligands / Supramolecular chemistry / Luminescence

Two functional, flexible ligands, namely 3,6-dipyrazolyl-9-ethylcarbazole (**L¹**) and 3,6-diimidazolyl-9-ethylcarbazole (**L²**) have been synthesized and characterized and their coordination to various Ag^{I}, Cd^{II}, and Co^{II} salts investigated. Six new complexes, **1**–**6**, have been obtained and fully characterized by IR spectroscopy, elemental analysis, and single-crystal X-ray diffraction. The 2D double helix framework of the complex $[CdL^{1}I_2]_n$ (**1**) is formed by C–H···I hydrogen bonds, whereas the same 2D double helix framework of compound $[\{AgL^{1}SO_3PhCH_3\}_2(CH_3OH)(H_2O)]_n$ (**2**) is formed by S–O···H and C–H···O hydrogen bonds and weak π–π interactions. The coordination modes of Cd^{II} and Co^{II} in $[CdL^{2}_2(NCS)_2]_n$(**3**),$[CoL^{2}_2(NCS)_2(CHCl_3)_2]_n$(**4**),$[CdL^{2}_2(NO_3)_2(CH_3OH)_2]_n$ (**5**), and $[CoL^{2}_2(NO_3)_2(CH_3OH)_2]_n$ (**6**) are the same, but in the packing diagram interlayers form a 3D network through C–H···S interactions and π–π interactions in **3**, interlayers form a 3D network through S···S interactions and π–π interactions in **4**, novel 3D structures are formed by interchain O···H–C hydrogen bonding and interlayer O···H–C hydrogen-bonding and π–π interactions in **5** and **6**. The structural differences between these complexes show the influence of the orientation of the coordinating group of the ligand. These results also show that the metal ion, anion, and nonbonding and π–π interactions are significant factors in controlling the structural topology of these metal-organic supramolecular architectures. In addition, the luminescence properties of **L¹**, **1**, **L²**, and **3** are investigated in the solid state at room temperature.

Introduction

Much recent work has been devoted to the design, synthesis, and structural characterization of novel multidimensional metal-organic frameworks (MOFs),[1–3] with the increasing volume of research being reflected in the exponential growth of the number of structures reported over the past few years. These structures are assembled by very strong and highly directional coordinative interactions, nonbonding weak interactions, and π–π interactions and display properties related to both the pure organic and inorganic compounds. The motivation behind such research lies in the large variety of peculiar architectures, together with the various potential applications of these compounds as functional materials (e.g., porosity allied with guest exchange, catalysis, gas storage, photoluminescence, nonlinear optical properties, chirality, clathration abilities, and magnetic properties).[4,5]

Biimidazole and bipyrazole have been widely used as biomimetic ligands in bioinorganic chemistry,[6] bridging ligands in organometallic chemistry for catalysis,[7] antitumor drugs,[8] and as building blocks of multidimensional MOFs due to their ability to coordinate to several metal centers in various modes.[9] However, it is difficult to model the structural and functional aspects of these complexes. It is well known that organic ligands with special functionality for use in supramolecular architectures have rarely been reported to date due to the synthetic difficulties involved. We expected to be able to combine such functionality by coordination using the ligands 9-ethyl-3,6-dipyrazolylcarbazole (**L¹**) and 9-ethyl-3,6-diimidazolylcarbazole (**L²**; Scheme 1). As imidazole[10] and pyrazole are electron-rich aromatic compounds, we introduced imidazolyl or pyrazolyl groups at the carbazole ring, in high yield, by a two-step Ullmann reaction. This functionalization of the organic molecule (addition of donor atoms such as N or O) allows its incorporation into inorganic coordination complexes, which have the advantage of higher thermal stability and solvent resistance than organic materials. Compared with our previous reports concerning 9-ethyl-3,6-bis[2-(2-pyridyl)ethenyl]carbazole and 9-ethyl-3,6-bis[2-(4-pyridyl)ethenyl]carbazole,[11]

[a] Department of Chemistry, Anhui University,
Hefei 230039, P. R. China
E-mail: zhpzhp@263.net
yptian@ahu.edu.cn
[b] State Key Laboratory of Crystal Materials, Shandong University,
Jinan, 250100, P. R. China
[c] State Key Laboratory of Coordination Chemistry, Nanjing University,
Nanjing 210093, P. R. China

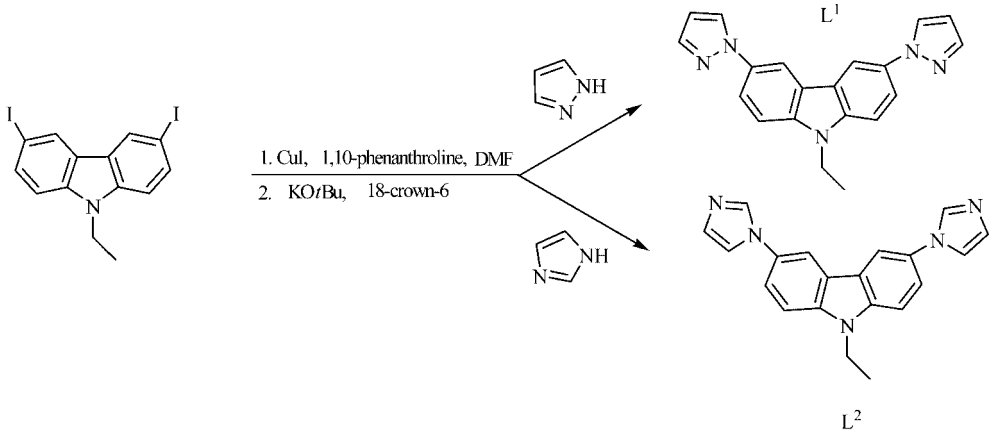

Scheme 1. Synthesis of ligands **L¹**, and **L²**.

replacement of the two pyridylethene groups with two imidazolyl or pyrazolyl groups enhances the flexibility of the ligand greatly. These ligands have a greater number of possible coordination modes than their more rigid analogs due to their flexibility and low symmetry since they can adopt different orientations according to the geometric needs of different metal ions. As a result of a systematic study of these ligands, this paper will describe a series of novel 2D and 3D coordination polymers with intermolecular weak non-bonding and π–π interactions and their photoluminescence properties. All the compounds have been characterized by IR spectroscopy, elemental analysis, and X-ray crystallography. In addition, the luminescence properties of the ligands and complexes **1** and **3** in the solid state are investigated.

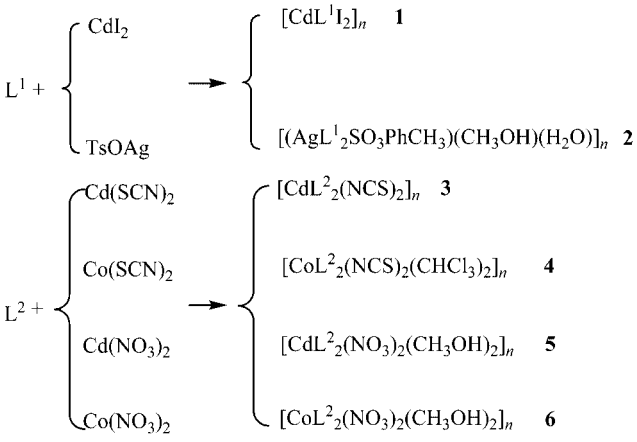

Scheme 2. Summary of the reactions between ligands and transition-metal salts.

Results and Discussion

We synthesized the ligands 9-ethyl-3,6-dipyrazolylcarbazole and 9-ethyl-3,6-diimidazolylcarbazole in good yield by a ligand-accelerated catalytic Ullmann reaction. The Ullmann reaction of aryl halides with amines or heterocycles is traditionally carried out by heating the reagent with copper powder in the presence of a base such as sodium carbonate or hydroxide.[12] However, we found that the Ullmann reaction of 9-ethyl-3,6-diiodocarbazole and imidazole or pyrazole could not be carried out under these conditions. Fortunately, addition of 1,10-phenanthroline and 18-crown-6 allowed **L¹** and **L²** to be synthesized in 84% and 79% yield, respectively.

Crystal Structures

The ligands react readily with a variety of Cd^{II}, Co^{II}, and Ag^{I} salts to form complexes **1**–**6**, which were fully characterized by IR spectroscopy, elemental analysis, and single-crystal X-ray diffraction. The general reaction is shown in Scheme 2. The coordination of Cd^{II} and Ag^{I} salts to **L¹** produced 2D polymer chains **1** and **2**, while the coordination of Cd^{II} and Co^{II} salts to **L²** produced the 3D polymers **3**–**6**.

Crystal Structure of $[CdL^1I_2]_n$ (1)

Single-crystal X-ray diffraction analysis revealed that the structure of the complex presents unusual double helices, as depicted in Figure 2 below. Further crystallographic details are given in the Experimental Section, and selected bond lengths and angles are listed in Table 1. It can clearly be seen from Figure 1 that the cadmium(II) ion displays a distorted tetrahedral geometry with two nitrogens from two L^1 ligands and two iodines in the coordination sphere. The bond angles around Cd(1) are in the range 99.73(16)–119.22(3)°, and the bond lengths between the Cd^{II} center and nitrogen range from 2.288(6) to 2.309(6) Å. The two pyrazolyl rings of each L^1 ligand have opposite orientations in complex **1**, and the pyrazolyl rings of the two independent L^1 ligands are twisted to meet the requirements of steric hindrance, with the dihedral angles between the pyrazolyl rings and the corresponding carbazolyl rings linked to them being 44.5° and 53.3°. Furthermore, the dihedral angle between the pyrazolyl rings in L^1 is 64.1°.

The helical polymer is composed of $[CdL^1I_2]$ monomers. A loose, single-stranded helical chain is formed by self-assembly of $[CdL^1I_2]$ by coordination of the metal-bound peripheral pyrazole-N of this unit to the neighboring Cd^{II}

Table 1. Selected intra- and intermolecular bond lengths [Å] and angles [°] for **1**–**6**. Symmetry operation used to generate equivalent atoms: **1**: A: $x + 1/2, -y + 1/2, -z$. **2**: A: $-x, y + 1/2, -z + 1/2$. **3**: A: $-x, -y, -z$. **4**: A: $-x, -y, -z$; B: $-x + 1/2, y + 1/2, -z + 1/2$; C: $x - 1/2, -y - 1/2, z - 1/2$. **5**: A: $-x, -y, -z$; B: $x + 1/2, y + 1/2, z$; C: $-x + 1/2, -y + 1/2, -z$. **6**: A: $-x, -y, -z$; B: $x + 1/2, y + 1/2, z$; C: $-x + 1/2, -y + 1/2, -z$.

		1	
Cd(1)–I(1)	2.7151(8)	N(3)–Cd(1)–I(1)	111.11(18)
Cd(1)–I(2)	2.7189(8)	N(5A)–Cd(1)–I(2)	105.67(14)
Cd(1)–N(3)	2.309(6)	N(3)–Cd(1)–I(2)	99.73(16)
Cd(1)–N(5A)	2.288(6)	N(5A)–Cd(1)–N(3)	100.7(2)
N(5A)–Cd(1)–I(1)	117.49(13)	I(1)–Cd(1)–I(2)	119.22(3)
		2	
Ag(1)–O(1)	2.467(14)	N(5A)–Ag(1)–N(3)	152.3(6)
Ag(1)–N(3)	2.19(2)	N(5A)–Ag(1)–O(1)	102.7(6)
Ag(1)–N(5A)	2.056(16)	N(3)–Ag(1)–O(1)	97.6(5)
Ag(2)–O(4)	2.539(15)	N(8)–Ag(2)–N(10A)	151.3(6)
Ag(2)–N(8)	2.17(2)	N(8)–Ag(2)–O(4)	112.4(5)
Ag(2)–N(10A)	2.274(14)	N(10A)–Ag(2)–O(4)	93.6(5)
		3	
Cd(1)–N(1)	2.345(2)	N(5)–C(11)	1.363(4)
Cd(1)–N(5)	2.322(3)	C(11)–C(13)	1.342(5)
Cd(1)–N(6)	2.347(3)	N(5A)–Cd(1)–N(5)	180.00(3)
N(1)–C(8)	1.313(4)	N(5)–Cd(1)–N(1)	90.25(9)
N(1)–C(19)	1.362(4)	N(5A)–Cd(1)–N(1)	89.75(9)
N(2)–C(8)	1.349(4)	N(1)–Cd(1)–N(1A)	180.0
N(2)–C(14)	1.366(4)	N(5A)–Cd(1)–N(6)	91.41(12)
C(14)–C(19)	1.359(5)	N(5)–Cd(1)–N(6)	88.59(12)
N(4)–C(17)	1.340(4)	N(1)–Cd(1)–N(6)	91.04(11)
N(4)–C(13)	1.365(4)	N(1)–Cd(1)–N(6A)	88.96(11)
N(5)–C(17)	1.313(4)	N(6)–Cd(1)–N(6A)	180.0
		4	
Co(1)–N(1)	2.128(3)	N(5)–C(6)	1.376(5)
Co(1)–N(4C)	2.144(3)	C(6)–C(7)	1.351(6)
Co(1)–N(2A)	2.161(3)	N(1)–Co(1)–N(1A)	180.0
N(2)–C(2)	1.318(5)	N(1)–Co(1)–N(4B)	90.97(12)
N(2)–C(4)	1.368(5)	N(1A)–Co(1)–N(4B)	89.03(12)
N(3)–C(2)	1.350(5)	N(4B)–Co(1)–N(4C)	180.0
N(3)–C(3)	1.372(5)	N(1)–Co(1)–N(2A)	89.66(12)
C(3)–C(4)	1.344(5)	N(1)–Co(1)–N(2)	90.34(12)
N(4)–C(5)	1.311(5)	N(4C)–Co(1)–N(2A)	87.92(11)
N(4)–C(7)	1.364(5)	N(4B)–Co(1)–N(2A)	92.08(11)
N(5)–C(5)	1.352(5)	N(2A)–Co(1)–N(2)	180.00(5)
		5	
Cd(1)–O(1)	2.258(10)	N(5)–C(4)	1.361(9)
Cd(1)–N(2)	2.307(7)	C(5)–C(6)	1.337(12)
Cd(1)–N(4B)	2.328(6)	O(1A)–Cd(1)–O(1)	180.000(2)
N(2)–C(1)	1.280(10)	O(1A)–Cd(1)–N(2)	94.1(4)
N(2)–C(3)	1.360(12)	O(1)–Cd(1)–N(2)	85.9(4)
N(3)–C(2)	1.335(10)	N(2)–Cd(1)–N(2A)	180.000(1)
N(3)–C(1)	1.356(10)	O(1A)–Cd(1)–N(4B)	94.3(4)
C(2)–C(3)	1.406(12)	O(1)–Cd(1)–N(4B)	85.7(4)
N(4)–C(4)	1.293(9)	N(2)–Cd(1)–N(4B)	85.8(2)
N(4)–C(6)	1.389(11)	N(2A)–Cd(1)–N(4B)	94.2(2)
N(5)–C(5)	1.345(10)	N(4B)–Cd(1)–N(4C)	180.000(1)
		6	
Co(1)–N(2)	2.117(5)	N(5)–C(5)	1.353(8)
Co(1)–O(1)	2.182(5)	C(5)–C(6)	1.318(9)
Co(1)–N(4B)	2.121(5)	N(2A)–Co(1)–N(2)	180.0(3)
N(2)–C(1)	1.318(7)	N(2)–Co(1)–N(4B)	93.27(18)
N(2)–C(3)	1.364(8)	N(2)–Co(1)–N(4C)	86.73(18)
N(3)–C(1)	1.350(7)	N(4B)–Co(1)–N(4C)	180.0(3)
N(3)–C(2)	1.375(7)	N(2A)–Co(1)–O(1)	89.9(2)
C(2)–C(3)	1.350(9)	N(2)–Co(1)–O(1)	90.1(2)
N(4)–C(4)	1.317(7)	N(4B)–Co(1)–O(1)	92.8(2)
N(4)–C(6)	1.374(8)	N(4C)–Co(1)–O(1)	87.2(2)
N(5)–C(4)	1.347(7)	O(1)–Co(1)–O(1A)	180.0(4)

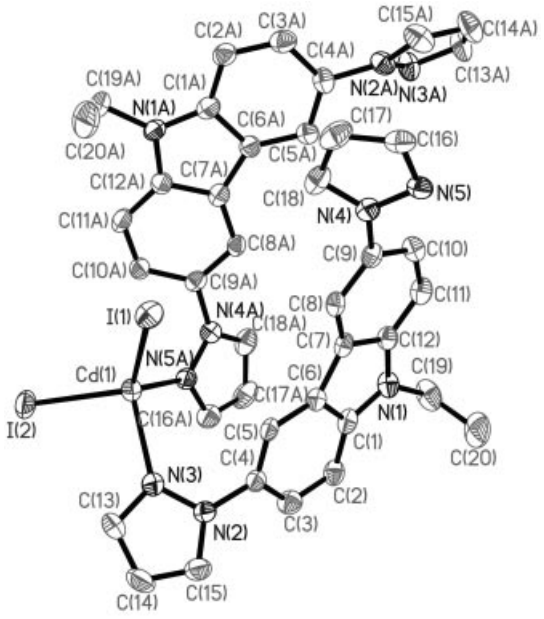

Figure 1. ORTEP diagram showing the structure of compound **1** with thermal ellipsoids at the 50% probability level and the atom-labeling scheme. Hydrogen atoms have been omitted for clarity.

center running along the *a* direction with a long pitch of about 3.819 Å (distance between two Cd centers with the same phase). At the widest point the diameter of the helix is 8.990 Å. The adjacent helical chains in $[CdL^1I_2]_n$, one of which is left-handed and the other right-handed, are not entangled but interact through C–H···I interactions (H···I 3.207 Å, ∠C–H···I 156.2°) between two helical chains to generate a very loose double-stranded helical chain [Figure 2(b)]. To illustrate this more clearly, the left- and right-handed helical chains are represented in Figures 2(a) and (c), respectively. These double-stranded helical chains are further extended into a two-dimensional architecture by C–H···I (H···I 3.207 Å, ∠C–H···I 156.2°; H···I 3.135 Å, ∠C–H···I 175.2°) interactions along the *b* axis (Figure 3). Taking the van der Waals radii of H and I to be 1.20 and 2.15 Å, respectively, any H···I contact of less than 3.35 Å and C–H···I angle greater than 130° can therefore be considered as being significant.[13–15] Because left- and right-handed helical chains coexist in the crystal structure, the whole crystal is mesomeric and does not exhibit chirality.

Crystal Structure of $[\{AgL^1SO_3PhCH_3\}_2(CH_3OH)(H_2O)]_n$ (2)

The structure of complex **2** consists of a novel two-dimensional double helical chain. As depicted in Figure 4, the structure of **2** reveals that the asymmetric unit contains two crystallographically and conformationally inequivalent molecules (a) and (b). Each silver(I) center is three-coordinate to two nitrogen donors of two independent L^1 ligands [Ag(1)–N(3) 2.19(2) Å, Ag(1)–N(5A) 2.056(16), Ag(2)–N(8)

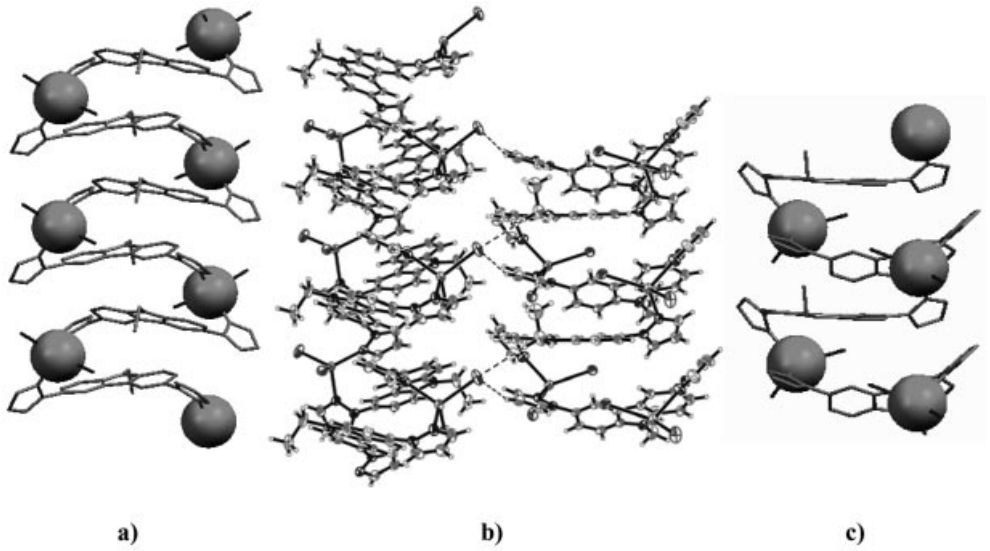

Figure 2. Ball-and-stick model of **1**. Cd atoms are given as balls and H atoms have been omitted for clarity. (a) Left-handed chain and (b) ball-and-stick plot of the double helix bridged by C–H···I interactions (dotted lines) in complex **1**; (c) right-handed chain.

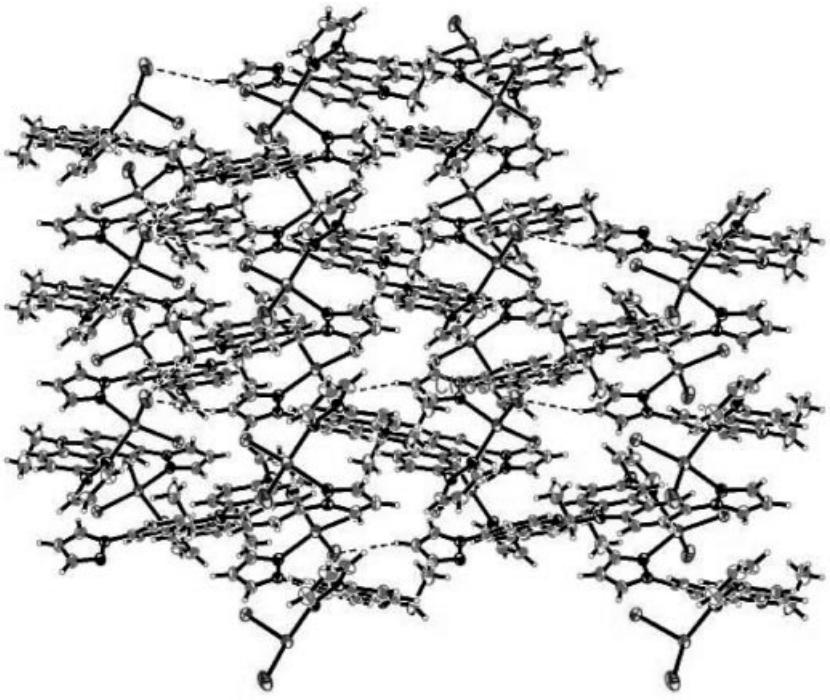

Figure 3. 2D network viewed along the *ab* plane in complex **1** showing C–H···I interactions as dotted lines.

2.17(2), Ag(1)–N(10A) 2.274(16) Å] and one oxygen atom of one *p*-toluenesulfonate anion [Ag(1)–O(1) 2.467(14), Ag(1)–O(4) 2.539(15) Å] to form a distorted trigonal geometry. The two pyrazolyl rings of L^1 also exhibit opposite orientations in complex **2**. These components connect to form an infinite polymeric chain structure similar to complex **1**. The dihedral angle between the two pyrazolyl rings of L^1 is about 71.4° or 108.6° and the dihedral angles between pyrazolyl rings and the corresponding carbazolyl rings linked to them are 57.6° and 43.0° in the Ag(1) chain. The dihedral angle between the two pyrazolyl rings of L^1 is about 73.9° or 106.1° and the dihedral angles between the pyrazolyl rings and the corresponding carbazolyl rings linked to them are 42.3° and 63.0° in the Ag(2) chain. Two loose single-stranded helical chains are formed by self-assembly of $[AgL^1{}_2SO_3PhCH_3]$ through coordination of the *meta*-bound peripheral pyrazole-N of this unit to the neighboring Ag^I center running along the crystallographic 2_1 axis in the *b* direction with a long pitch of about 5.3385 Å; at the widest point the diameter of the helix is 8.7711 Å.

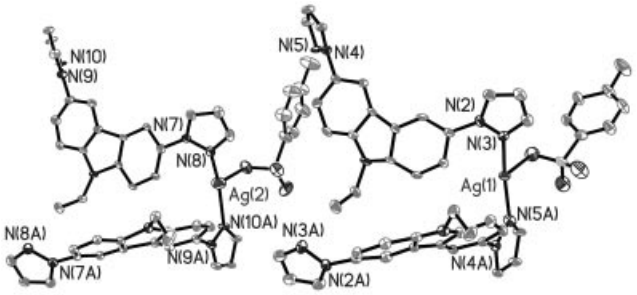

Figure 4. ORTEP diagram showing the structure of compound **2** with thermal ellipsoids at the 50% probability level. H atoms and water and methanol molecules have been omitted for clarity.

In addition, like complex **1**, the adjacent helical chains in compound **2**, one of which is left-handed and the other right-handed, are not entangled together but interact through an S–O···H interaction (H···O 2.469 Å, ∠ S–O···H 136.5°), which alternates between the two helical chains to generate a loose, double-stranded helical chain. Taking the van der Waals radii of H and O to be 1.20 and 1.40 Å, respectively, any H···O contact less than 2.60 Å and S–O···H angle above 130° can be considered to be significant. To illustrate this clearly, the left- and right-handed helical chains are represented in Figure 5. Like complex **1**, these double-stranded helical chains are further extended into a two-dimensional architecture by O···H–C hydrogen-bond interactions between the ligands and oxygen atoms of adjacent chains (O···H 2.455 Å, ∠ O···H–C 152.1°) and a very weak π–π stacking interaction (the shortest distance between carbazolyl rings is 4.3477 Å) along the *a* axis in compound **2** (Figure 6). The whole crystal is mesomeric and does not exhibit chirality, just like compound **1**.

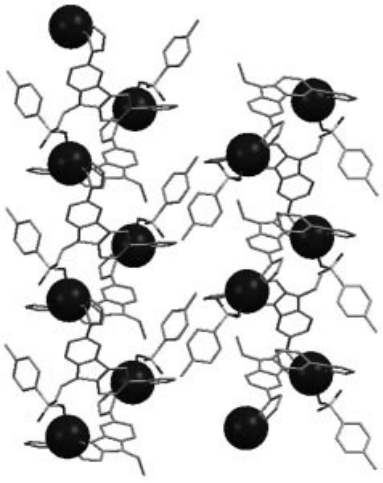

Figure 5. A ball-and-stick model of complex **2** showing the helicity. Ag atoms are given as balls and H atoms and water and methanol molecules have been omitted for clarity.

Crystal Structure of $[CdL^2_2(NCS)_2]_n$ (3)

The coordination environment of the Cd^{II} ion in complex **3** is shown in Figure 7. Each Cd^{II} center, which is located at an inversion center, is in an octahedral environment com-

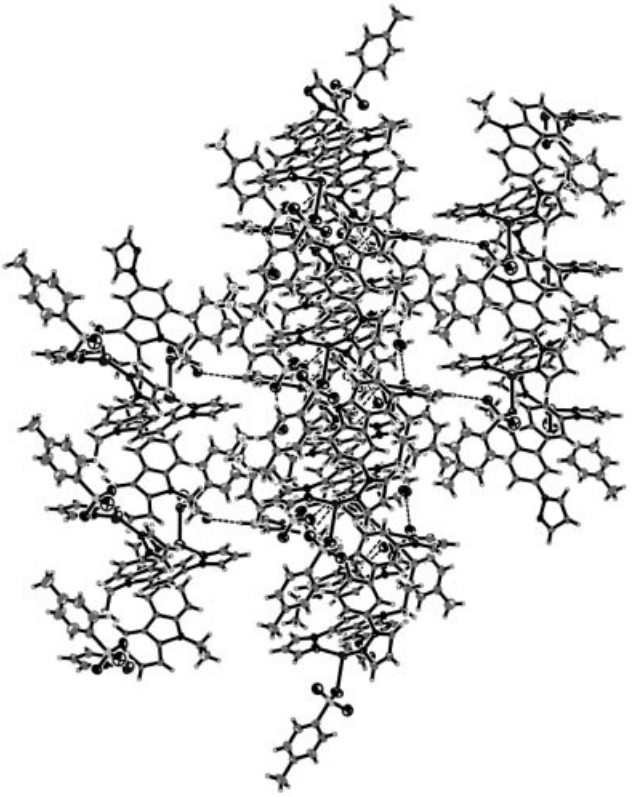

Figure 6. 2D network viewed along the *ab* plane in compound **2** showing the π–π stacking interactions and S–O···H and C–H···O interactions (dotted lines); the shortest H···O interaction is 2.455 Å.

posed of two nitrogen atoms from two NCS^- groups in the axial positions and four imidazolyl nitrogen atoms from four L^2 molecules in the equatorial plane. The Cd–N_{NCS} [2.347(3) Å] bond length is longer than Cd–N_{im} [Cd–N(1) 2.345(2), Cd–N(5) 2.323(3) Å], and N–Cd–N bond angles with the same orientational fall in the range 88.59(12)–91.04(11)°. The two terminal NCS^- groups are bent, with a

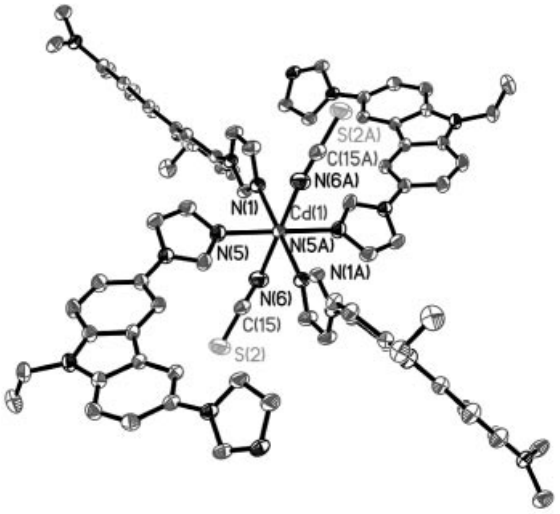

Figure 7. Octahedral coordination geometry around the cadmium center in **3**.

Cd(1)–N(6)–C(15) bond angle of 140.4(3)°, and are coordinated axially in opposite directions. The two imidazolyl rings within each ligand deviate from coplanarity, the dihedral angles between each terminal imidazolyl ring and the central carbazole unit being 139.8° and 31.4°.

The two imidazolyl rings of L^2 in complex **3** adopt the same orientation, the dihedral angle between two imidazolyl rings being 54.3°, and each one bridges two Cd^{II} centers to form a 2D sheet containing $[Cd_4L^2_4]$ macrocycles as subunits. The Cd^{II} atoms lie at the nodes of a rhombic grid in the undulating $[CdL^2_2(NCS)_2]_n$ layer, with ligand-bridging Cd···Cd distances of 23.744 and 12.769 Å (Figure 8). Each layer contains π–π interactions (the shortest distance between parallel carbazole rings is 3.89 Å), and these layers are stacked by C–H···S (H···S 2.913 Å) interactions along the *c* axis (Figure 9) to form a 3D network. Taking the van der Waals radii of H and S to be 1.00 and 2.05 Å, respectively, any H···S contact less than 3.05 Å can be considered significant. The H···S distance of 2.913 Å indicates the formation of C–H···S hydrogen bonds. C–H···S hydrogen-bonding interactions are very important in several novel supramolecular structures.[16]

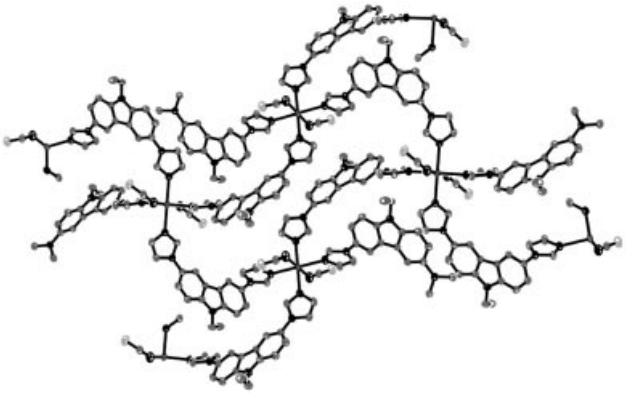

Figure 8. Two-dimensional grid structure of **3**.

Crystal Structure of $[CoL^2_2(NCS)_2(CHCl_3)_2]_n$ (4)

The coordination environment of the Co^{II} ion in **4** is shown in Figure 10. Each metal center is six-coordinate to two NCS groups and four L^2 ligands. The Co–N bond involving the NCS group [Co–N_{NCS} 2.128(3) Å] is shorter than the other Co–N bonds [2.144(3) and 2.161(3) Å]. It is clear that each Co^{II} center lies in the same octahedral coordination environment as complex **3**, and N–Co–N angles with the same orientation lie in the range 87.92(11)–92.08(11)°, similar to that for Cd^{II}. The oppositely oriented N–Co–N bond angles for NCS^- and the L^2 ligands are 180°. The NCS ligands are coordinated axially in a terminal mode with angles of 180°. The two imidazolyl rings within each L^2 deviate by 50.2° and 140.7°, respectively, from the carbazole plane. The two imidazolyl rings of L^2 in complex **4** also adopt the same orientation and their dihedral angle is 65.0°. Selected bond lengths and angles for **4** are listed in Table 1.

Figure 11 shows the lamellar network of **4** in which the adjacent Co^{II} centers are linked by a bridging L^2 ligand in two different directions to form large and nearly square repeating grids (the ligand-bridging Co···Co distances are 12.492 and 20.845 Å) in a 2D sheet. Each sheet contains weak π–π interactions[17] (the shortest distance between parallel carbazole rings is 4.225 Å), and these sheets are stacked by π–π (the shortest distance between parallel carbazole rings is 3.753 Å) and S···S (S···S 3.589 Å) interactions along the *a* axis (Figure 12) to form a 3D network. Taking the van der Waals radii of S to be 2.05 Å, any S···S contact less than 4.10 Å and C–S···S angle greater than 130° may therefore potentially be considered significant. The S···S distance of 3.589 Å and C–S···S angle of 153.2° in complex **4** indicate such an S···S interaction. In general, weak S···S interatomic interactions are often observed in multi-sulfur systems,[18] and these S···S weak interactions in complex **4** construct a novel supramolecular network structure. The shortest intersheet Co···Co distance is 13.139 Å. The coordination environment of the metal ions is similar

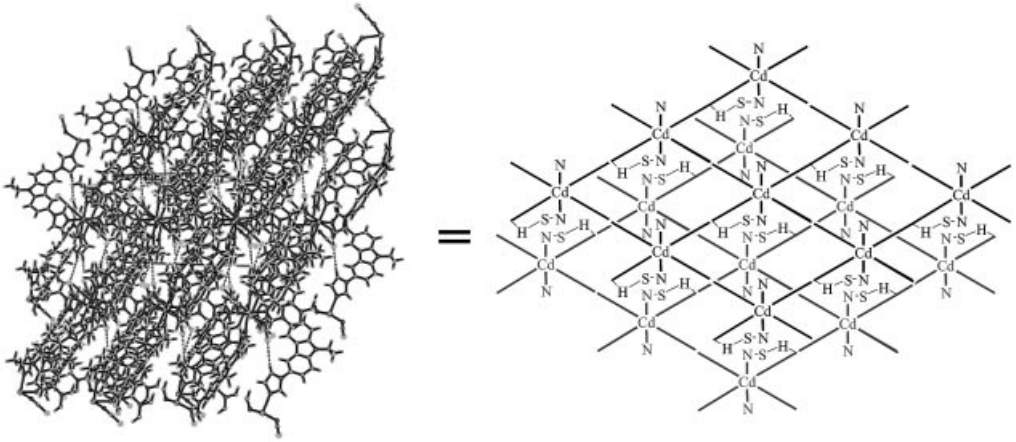

Figure 9. Molecular packing viewed along the *c* axis showing the intermolecular hydrogen bond C–H···S and π–π interactions.

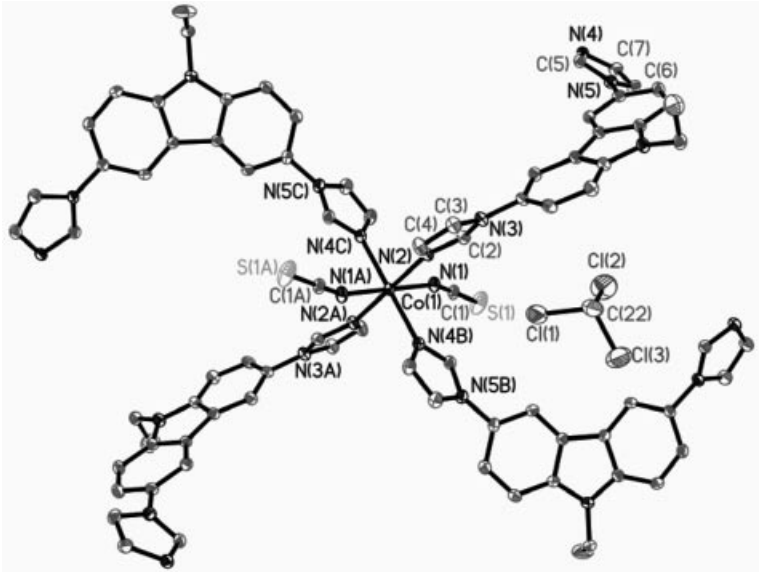

Figure 10. Octahedral coordination geometry around the cobalt center in **4**.

to that in complex **3**, but they adopt a different stacking arrangement due to the presence of different metal ions.

Crystal Structure of $[CdL^2_2(NO_3)_2(CH_3OH)_2]_n$ (5)

The crystallographic analysis of complex **5** revealed that its structure is a 1D polymeric chain structure which is constituted by $[CdL^2_2(NO_3)_2]$ units. As shown in Figure 13, the Cd^{II} atoms reside on crystallographic inversion centers and each has a slightly distorted octahedral $[CdN_4O_2]$ coordination geometry with the equatorial sites occupied by imidazolyl nitrogen donors from L^2; the axial positions are occupied by two monodentate nitrate counterions. The Cd–N and Cd–O bonds fall in the range of 2.307(7)–2.328(6) Å and 2.258(10) Å, respectively, which are very close to the corresponding bond lengths found in $[Cd(NO_3)_2(L)_2]$ [L = 2,5-bis(3-pyridyl)-3,4-diaza-2,4-hexadiene].[7] Two imidazolyl rings of L^2 also adopt the same orientation with a dihedral angle of 67.9°.

Compound **5** adopts a chain motif in the solid state with the Cd^{II} centers linked by four crystallographically equiva-

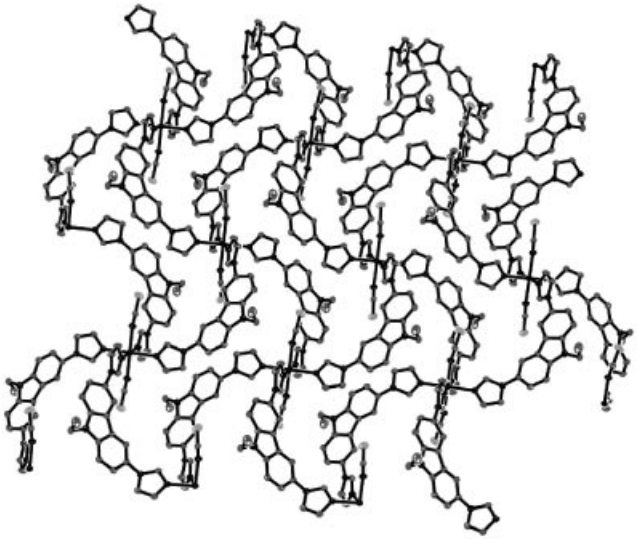

Figure 11. Two-dimensional grid structure of **4**.

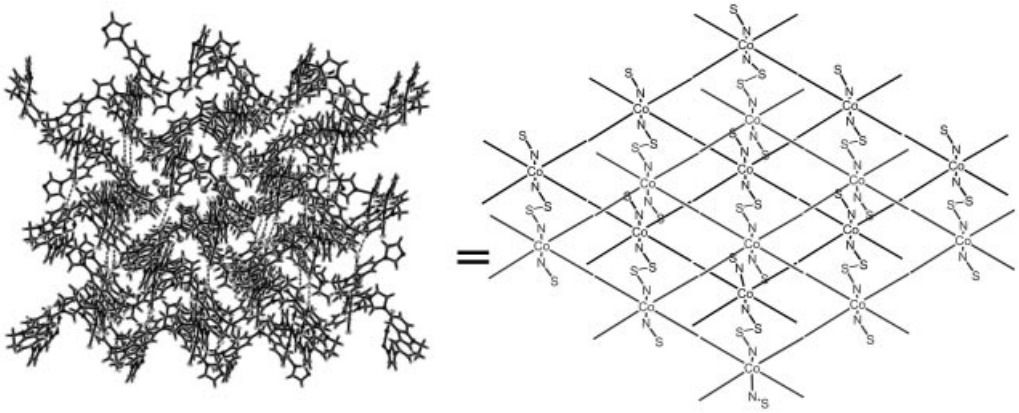

Figure 12. Molecular packing viewed along the *c* axis showing the intermolecular S···S and π–π interactions (dotted lines).

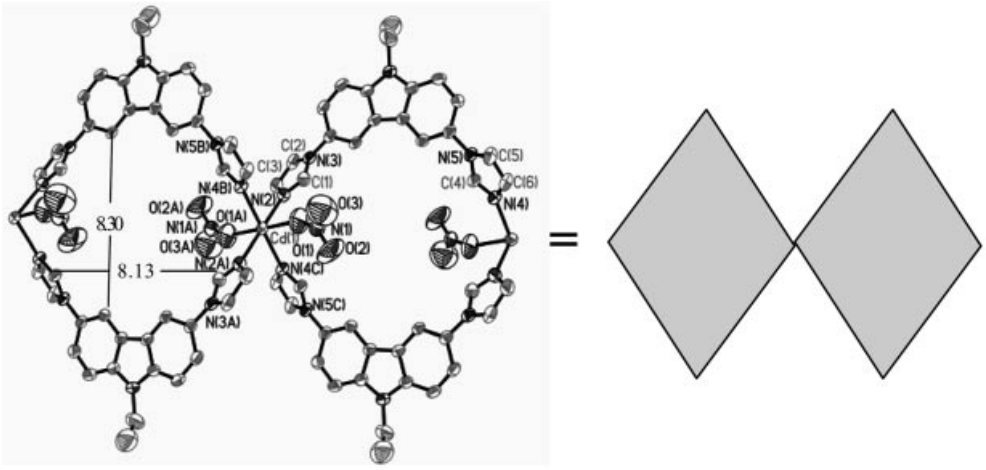

Figure 13. View of the basic box unit in the polymer chains of **5** (methanol molecules have been omitted for clarity).

lent L^2 ligands into an undulating one-dimensional chain running along the *b* axis (Figure 14). As shown in Figure 13, the individual "links" in the chain consist of M_2L_2 units, which a form 26-membered ring. The approximate (crystallographic) dimensions of the rings are 8.13×8.30 Å^2 (Figure 13). The intra- and interchain Cd···Cd distances are both 11.861 Å. Two crystallographically equivalent monodentate NO_3^- ions are located above and below the M_2L_2 ring planes. In addition, hydrogen-bonding interactions between the chains, involving one uncoordinated O of the monodentate nitrate ion and H on the methyl and ethyl group of a ligand in an adjacent chain, are present in **5** (Figure 15). The O···H contacts are 2.498 and 2.534 Å. The existence and structural importance of weak C–H···O hydrogen-bonding interactions are now well established and they are present in many molecular and polymeric compounds.[19–22] O···H–C hydrogen bonds, although they are weak and are accompanied by π–π interactions (the shortest distance between parallel carbazolyl rings is 3.685 Å), contribute significantly to the structural organization of **5** in the crystalline phase, giving rise to a two-dimensional arrangement in which one-dimensional chains align together in a shoulder-to-shoulder fashion to generate a 2D sheet along the *a* axis. It is very interesting that these sheets are stacked to form a 3D structure along the *c* axis by intersheet hydrogen-bonding interactions and π–π interactions (the shortest distance between parallel carbazolyl rings is 3.4791 Å). Figure 16 shows that these sheets are overlapped vertically by the other uncoordinated O of the monodentate nitrate ion and two H atoms of the phenyl group of a ligand in the other sheet (the O···H contacts are 2.460 and 2.475 Å, respectively).

The metal ion in this complex is the same as in complex **3** but the anion is different, which indicates that the nature of the anion is a significant factor in controlling the structural topology of these metal-organic supramolecular architectures and offers the opportunity to control the coordination networks by changing the anion.

Crystal Structure of $[CoL^2{}_2(NO_3)_2(CH_3OH)_2]_n$ (6)

In general, all the Co^{II} centers in the coordination polymers generated from cobalt nitrate and *N*,*N*′-bidentate ligands adopt a $\{CoN_3O_4\}$ coordination environment.[22] zur Loye[19] reported the first $\{CoN_4O_2\}$ coordination sphere in coordination polymers. Compound **6** reported here also has a $\{CoN_4O_2\}$ coordination sphere and is similar to compound **5**. One of the Co–N bond lengths is 2.117(5) Å, which is significantly shorter than the corresponding Co–N bond lengths [2.210(2)–2.261(2) Å] in the $\{CoN_4N'_2\}$ coordination spheres but is consistent with the Co–N bond lengths in a $\{CoN_3O_4\}$ coordination sphere.[23] The two imidazolyl rings of the ligand also adopt the same orientation, with a dihedral angle of 69.4°.

Compound **6** is isostructural with **5** except that the Cd^{II} centers are replaced by Co^{II} atoms. The intra- and interchain Co···Co distances are both 11.72 Å. The same interchain hydrogen-bonding system is present in **6** (O···H 2.27, O···C 2.939 Å; O···H–C 125.9°) and π–π interactions

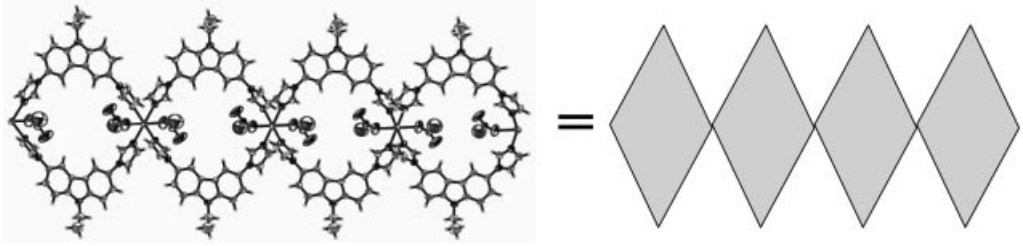

Figure 14. 1D chain in **5**.

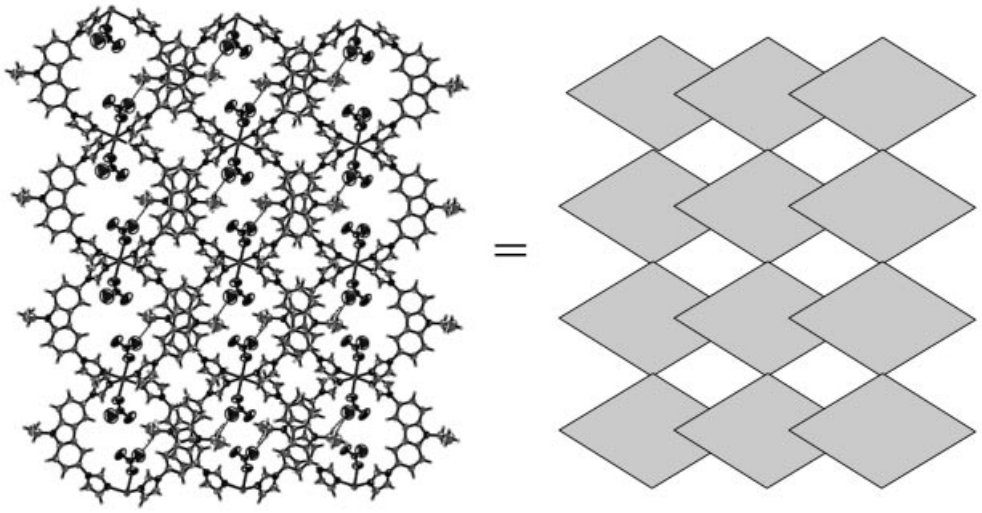

Figure 15. A view of the 2D networks formed by adjacent 1D chains in **5** showing the C–H···O hydrogen-bonding system and π–π interactions (dotted lines).

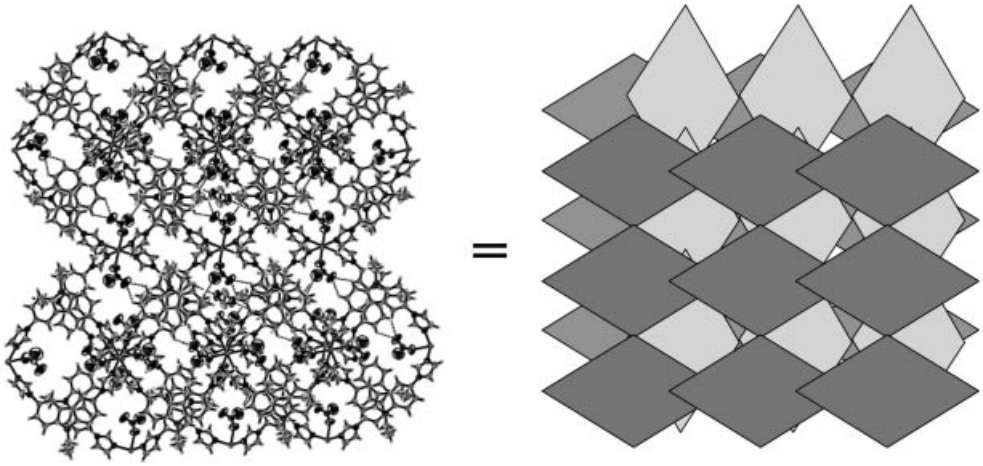

Figure 16. A view of the 3D network formed by interlayer C–H···O hydrogen bonding and π–π interactions (dotted lines).

(the shortest distance between parallel carbazolyl rings is 3.743 Å). The same intersheet hydrogen-bonding system is also present in **6** (O···H 2.56 and 2.514 Å; O···C 3.153 and 3.12 Å; O···H–C 122.0° and 123°) and π–π interactions (the shortest distance between parallel carbazolyl rings is 3.8135 Å). When compared with complex **4**, this complex again shows that the nature of the anion is a significant factor in controlling the structural topology of these metal-organic supramolecular architectures.

When the ligands of complexes **1**–**6** are compared, it can be seen that the two pyrazolyl rings of L^1 keep the same opposite orientation with a different dihedral angle during the complex formation (the dihedral angles of the two pyrazole rings are 64.1° for **1** and 71.4°, 73.9° for **2**) and the two imidazolyl rings of L^2 keep the same orientation with a different dihedral angle during the complex formation (the dihedral angles of the two imidazole rings are 54.3°, 65.0°, 67.9°, and 69.4° for **3**, **4**, **5**, and **6**, respectively). The opposite orientation and corresponding angle allow L^1 to coordinate the metal ion as a bidentate ligand using the nitrogen atom and form 1D helical chains, whereas the same orientation and corresponding angle allow L^2 to coordinate the metal ion as a bidentate ligand using the nitrogen atom and form a 2D grid or a 1D double chain. Finally, the intermolecular nonbonding weak interactions link low-dimensional entities into high-dimensional supramolecular frameworks.

In summary, two novel functional ligands and six coordination complexes (**1**–**6**) have been prepared and structurally characterized; the latter display metal-organic supramolecular architectures. As flexible bridging ligands can easily produce unique frameworks with useful properties due to their flexibility and orientational freedom,[24] we designed and synthesized conveniently two novel functional flexible ligands, namely 9-ethyl-3,6-dipyrazolylcarbazole and 9-ethyl-3,6-diimidazolylcarbazole, that are capable of coordinating to metal centers through their respective imidazolyl or pyrazolyl nitrogen atoms form novel 2D or 3D polymers. The results indicate that the metal ion, anion, and non-

Table 2. Crystallographic data and structure refinement for complexes **1**–**6**.

Complex	**1**	**2**	**3**	**4**	**5**	**6**
Empirical formula	$C_{20}H_{17}CdI_2N_5$	$C_{55}H_{54}Ag_2N_{10}O_8S_2$	$C_{42}H_{34}CdN_{12}S_2$	$C_{44}H_{36}Cl_6CoN_{12}S_2$	$C_{42}H_{42}CdN_{12}O_8$	$C_{42}H_{42}CoN_{12}O_8$
Formula mass	693.59	1262.95	883.33	1068.60	955.28	901.81
Crystal system	orthorhombic	monoclinic	monoclinic	monoclinic	monoclinic	monoclinic
Space group	$P2_12_12_1$	$P2_1/c$	$P2_1/c$	$P2_1/n$	$C2/c$	$C2/c$
a [Å]	7.6381(13)	28.199(7)	11.1196(15)	13.139(3)	17.341(5)	17.245(5)
b [Å]	17.050(3)	10.677(3)	12.7695(17)	12.492(2)	16.186(5)	15.876(5)
c [Å]	17.623(3)	19.036(4)	14.711(2)	14.902(3)	15.353(5)	15.436(4)
β [°]	90	102.798(13)	103.001(2)	95.838(3)	107.148(4)	106.503(4)
V [Å^3]	2295.0(7)	5589(2)	2035.3(5)	2433.1(8)	4118(2)	4052.1(19)
Z	4	4	2	2	4	4
$D_{calcd.}$ [g cm^{-3}]	2.007	1.490	1.441	1.459	1.541	1.478
θ_{range} [°]	2.31–25.01	2.20–25.01	2.14–25.00	1.97–25.10	1.76–25.09	1.78–25.10
Total data	12094	13706	10390	12529	10037	9503
Unique data	4022	4811	3583	4321	3508	3371
Number of refined parameters	253	696	260	296	286	287
R_1	0.0347	0.0295	0.0359	0.0560	0.0768	0.0769
wR_2	0.0820	0.0782	0.0892	0.1336	0.1952	0.1803
GOF	1.024	1.003	1.035	1.002	1.043	1.014

bonding and π–π interactions are significant factors in controlling the structural topology of these metal-organic supramolecular architectures.

Experimental Section

All chemicals and solvents were dried and purified by usual methods. Elemental analyses were performed with an Elmentar Vario EL-III analyzer. IR spectra were recorded with a Nicolet FT-IR Nexus 870 instrument in the range 4000–400 cm^{-1} by using KBr pellets. ^{1}H NMR spectra were recorded with a Bruker 600 MHz Ultrashield spectrometer and are reported in parts per million (ppm) from TMS (δ). Melting points were recorded with a Perkin–Elmer Pris-1 DMDA-V1 analyzer under N_2 at a heating rate of 5 °C min^{-1}. The luminescent spectra were recorded for single crystals at room temperature using a Fluorolog-3-TAU steady-state/lifetime spectrofluorometer. The excitation slit and the emission slit were 2.5 nm.

X-ray Crystallography: Single-crystal X-ray diffraction measurements were performed with a Bruker Smart 1000 CCD diffractometer equipped with a graphite crystal monochromator situated in the incident beam for data collection at room temperature. Unit cell parameters and data collections were performed with Mo-K_α radiation (λ = 0.71073 Å). Unit cell dimensions were obtained with least-squares refinements, and all structures were solved by direct methods using SHELXL-97.[26] The other non-hydrogen atoms were located in successive difference Fourier syntheses. The final refinement was performed by full-matrix least-squares methods with anisotropic thermal parameters for non-hydrogen atoms on F^2. The hydrogen atoms were added theoretically as riding on their parent atoms. Crystallographic crystal data and processing parameters for complexes **1**–**6** are given in Table 2. Selected bond lengths and bond angles are listed in Table 1.

CCDC-611826 (for **1**), -611825 (for **2**), -274291 (for **3**), -278330 (for **4**), -278332 (for **5**) and -278331 (for **6**) contain the supplementary crystallographic data for this paper. These data can be obtained free of charge from The Cambridge Crystallographic Data Centre via www.ccdc.cam.ac.uk/data_request/cif.

Preparation of 9-Ethyl-3,6-dipyrazolylcarbazole (L^1): CuI (0.27 g, 1.35 mmol), 1,10-phenanthroline (0.60 g, 3.02 mmol), and 3 mL of dmf were added to a three-necked flask equipped with a magnetic stirrer and a reflux condenser. This mixture was refluxed for 5 min in an oil bath at 120 °C, cooled to room temperature, and then pyrazole (3.65 g, 53.61 mmol), KO*t*Bu (6.05 g, 54.00 mmol), 9-ethyl-3,6-diiodocarbazole (3.00 g, 6.72 mmol),[11] and 18-crown-6 (little) were added and the mixture heated to 130 °C for 36 h. It was then cooled to room temperature and the residue was extracted with 150 mL of dichloromethane, washed three times with distilled water, and dried with anhydrous magnesium sulfate. It was then filtered and concentrated. Recrystallization from ethyl acetate produced light yellow crystals. Yield: 1.82 g (84%). M.p. 202–202.4 °C. ^{1}H NMR (600 MHz, [D$_6$]DMSO): δ = 1.35 (t, J = 7.20 Hz, 3 H, CH_3), 4.51 (q, J = 7.20 Hz, 2 H, CH_2), 6.57 (s, 2 H, phenyl), 7.75 (d, J = 8.40 Hz, 4 H, phenyl), 7.98 (d, J = 7.2 Hz, 2 H, pyrazolyl), 8.53 (d, J = 1.8 Hz, 2 H, pyrazolyl), 8.71 (d, J = 0.6 Hz, 2 H, pyrazolyl) ppm. $C_{20}H_{17}N_5$ (327.39): calcd. C 73.37, H 5.23, N 21.39; found C 73.67, H 5.40, N 21.16. IR (KBr): $\tilde{\nu}$ = 3141 (w), 2973 (m), 2937 (w), 1636 (m), 1618 (m), 1584 (w), 1509 (vs), 1483 (vs), 1392 (m), 1316 (s), 1223 (m), 1195 (m), 1153 (m), 1085 (w), 1046 (m), 936 (m), 881 (m), 835 (w), 799 (m), 750 (s), 664 (m), 615 (m) cm^{-1}.

Preparation of 9-Ethyl-3,6-diimidazolylcarbazole (L^2): L^2 was obtained by a similar method to **L^1**. Yield: 1.72 g (79%). M.p. 221–221.6 °C. ^{1}H NMR (500 MHz, [D$_6$]DMSO): δ = 1.34 (t, J = 7.04 Hz, 3 H, CH_3), 4.54 (q, J = 6.98 Hz, 2 H, CH_2), 7.15 (s, 2 H, imidazolyl), 7.79 (d, J = 8.72 Hz, 2 H, phenyl), 7.75 (t, J = 5.12 Hz, 4 H, phenyl), 8.22 (s, 2 H, imidazolyl), 8.50 (d, J = 1.36 Hz, 2 H, imidazolyl) ppm. $C_{20}H_{17}N_5$ (327.39): calcd. C 73.37, H 5.23, N 21.39; found C 73.30, H 5.19, N 21.07. IR (KBr): $\tilde{\nu}$ = 3104 (m), 2969 (w), 2863 (w), 1637 (m), 1620 (m), 1581 (m), 1506 (vs), 1380 (m), 1320 (m), 1260 (m), 1228 (m), 1105 (m), 1063 (m), 904 (m), 804 (m), 663 (m) cm^{-1}.

Preparation of $[CdL^1I_2]_n$ (1): 9-Ethyl-3,6-dipyrazolylcarbazole (**L^1**; 32.74 mg, 0.1 mmol) and CdI_2 (36.62 mg, 0.1 mmol) were dissolved in MeOH (10 mL). The mixture was refluxed for 2 h at 70 °C and then cooled to room temperature to give a clear colorless solution. Pale colorless crystals suitable for X-ray diffraction were obtained after two weeks by slow evaporation of the methanol solution at room temperature. Yield: 61.73 mg (89%). IR (KBr): $\tilde{\nu}$ = 3117 (m), 2971 (w), 2925 (w), 1632 (m), 1613 (m), 1519 (s), 1487 (s), 1403 (m), 1383 (m), 1230 (s), 1192 (m), 1149 (w), 1067 (m), 1038 (m),

958 (w), 894 (m), 874 (m), 805 (m), 746 (vs), 670 (w) cm^{-1}. $C_{20}H_{17}CdI_2N_5$ (693.59): calcd. C 34.63, H 2.47, N 10.10; found C 35.01, H 2.50, N 10.15.

Preparation of $\{[AgL^1SO_3PhCH_3]_2(CH_3OH)(H_2O)\}_n$ (2): Complex **2** was prepared by a procedure similar to that of **1** except that AgOTs (27.79 mg, 0.1 mmol) was dissolved in MeOH (10 mL) and H_2O (0.5 mL). Colorless transparent cube-shaped crystals of **2** suitable for X-ray structure determination were obtained in 81% yield. $C_{55}H_{54}Ag_2N_{10}O_8S_2$ (1263.0): calcd. C 52.31, H 4.31, N 11.09; found C 52.74, H 4.08, N 11.30. IR (KBr): $\tilde{\nu}$ = 3131 (w), 2978 (w), 2920 (w), 1629 (m), 1581 (m), 1516 (s), 1487 (s), 1404 (m), 1382 (m), 1351 (w), 1317 (m), 1188 (s), 1119 (m), 1064 (m), 1034 (m), 1007 (m), 814 (m), 763 (m), 677 (s), 615 (m), 565 (s) cm^{-1}.

Preparation of $[CdL^2_2(NCS)_2]_n$ (3): A solution of L^2 (65.48 mg, 0.20 mmol) in 5 mL of $CHCl_3$ solution was layered onto a solution of $Cd(SCN)_2$ (22.86 mg, 0.10 mmol) in MeOH (10 mL) and allowed to stand for ten days to give pale-yellow single crystals. Yield: 85% (75.08 mg). $C_{42}H_{34}CdN_{12}S_2$ (883.33): calcd. C 57.11, H 3.88, N 19.03; found C 56.89, H 3.68, N 18.67. IR (KBr): $\tilde{\nu}$ = 3130 (m), 2976 (w), 2933 (w), 2088 (vs), 2034 (s), 1621 (m), 1587 (m), 1508 (vs), 1388 (m), 1332 (m), 1303 (m), 1269 (m), 1228 (s), 1122 (m), 1065 (s), 924 (m), 873 (m), 808 (s), 736 (s), 659 (s) cm^{-1}.

Preparation of $[CoL^2_2(NCS)_2(CHCl_3)_2]_n$ (4): Complex **4** was prepared by a procedure similar to that for **3** but with $Co(SCN)_2$ (17.48 mg, 0.1 mmol) in place of $Cd(SCN)_2$. Yield: 89% (95.11 mg). $C_{44}H_{36}Cl_6CoN_{12}S_2$ (1068.6): calcd. C 49.45, H 3.40, N 15.73; found C 49.87, H 3.60, N 15.36. IR (KBr): $\tilde{\nu}$ = 3131 (m), 2977 (w), 2930 (w), 2076 (vs), 2033 (s), 1614 (w), 1585 (m), 1508 (vs), 1380 (m), 1330 (m), 1268 (m), 1229 (m), 1152 (w), 1123 (w), 1090 (w), 1064 (s), 935 (m), 833 (m), 809 (m), 744 (s), 661 (s) cm^{-1}.

Preparation of $[CdL^2_2(NO_3)_2(CH_3OH)_2]_n$ (5): Complex **5** was prepared by a procedure similar to that for **3** but with $Cd(NO_3)_2$ (34.60 mg, 0.1 mmol) instead of $Cd(SCN)_2$. Yield: 80% (76.42 mg). $C_{42}H_{42}CdN_{12}O_8$ (955.28): calcd. C 52.81, H 4.43, N 17.60; found C 52.98, H 4.05, N 17.38. IR (KBr): $\tilde{\nu}$ = 3134 (m), 2977 (w), 2928 (w), 1640 (w), 1615 (m), 1585 (w), 1515 (vs), 1405 (m), 1385 (vs), 1317 (s), 1272 (m), 1230 (m), 1143 (w), 1115 (m), 1066 (s), 931 (m), 873 (w), 809 (m), 742 (m), 659 (m), 663 (s) cm^{-1}.

Preparation of $[CoL^2_2(NO_3)_2(CH_3OH)_2]_n$ (6): Complex **6** was prepared by a procedure similar to that for **3** but with $Co(NO_3)_2$ (33.10 mg, 0.1 mmol) instead of $Cd(SCN)_2$. Yield: 85% (76.65 mg). $C_{42}H_{42}CoN_{12}O_8$ (901.81): calcd. C 55.94, H 4.69, N 18.64; found C 56.31, H 4.26, N 18.79.. IR (KBr): $\tilde{\nu}$ = 3142 (w), 2977 (w), 2929 (w), 1633 (w), 1581 (w), 1510 (vs), 1385 (vs), 1334 (m), 1309 (m), 1260 (m), 1231 (s), 1148 (w), 1117 (m), 1086 (m), 1063 (s), 965 (w), 937 (m), 866 (m), 811 (s), 742 (m), 660 (s) cm^{-1}.

Thermogravimetric Analysis: Complexes **2**, **4**, **5**, and **6** are unstable in air. Complexes **1** and **3** are stable under ambient conditions, and thermogravimetric experiments were performed on single-crystalline samples. The TG-DSC measurements of complexes **1** and **3** were determined in the range 20–800 °C under nitrogen. TG data show that **1** is stable up to 223 °C and then loses weight from 223 to 298 °C, corresponding to decomposition of ligand L^1. The final weight loss occurs at 543 °C. The TG data of **2** show that it is also stable up to 245 °C and then keeps losing weight from 245 °C to 301 °C, corresponding to decomposition of ligand L^2. The final weight loss occurs at 568 °C.

Luminescent Properties: Metal complexes are promising luminescent materials with potential applications as light-emitting materials (LEDs) owing to their ability to enhance, shift, and quench luminescent emission of organic ligands by metal coordination. The solid-state emission spectra of L^1, **1**, L^2, and **3** are shown in Figure 17(a) and (b). The nanosecond range of the lifetime in the solid state at 298 K reveals that the emission is fluorescent in nature. A comparison of the fluorescence spectra of L^1, **1**, L^2, and **3** suggests their emission origin. The solid-state fluorescent analyses show that the complexes exhibit different properties. Free L^1 exhibits an emission maximum at 414 nm with a shoulder peak at about 435 nm, which is completely invariant upon excitation in the range 270–369 nm; complex **1** presents a broad strong emission band with a maximum at 470 nm upon excitation in the range 275–383 nm, which can be tentatively assigned to a MLCT based on a significant red shift from L^1 to **1** and literature studies.[25] Free L^2 exhibits an emission maximum at 396 nm with a shoulder peak at about 412 nm, which is completely invariant upon excitation in the range 260–312 nm; complex **3** presents a sharp strong emission band with a maximum at 400 nm upon excitation in the range 268–362 nm, which is largely characteristic of an intraligand fluorescent emission. It is obvious that insoluble **1** and **3** possess strong fluorescent intensity, which suggests they may have potential applications in solvent-resistant fluorescent materials.

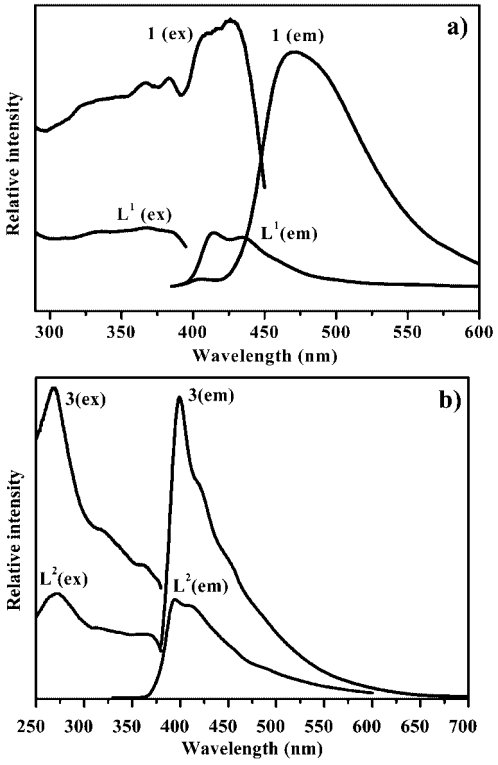

Figure 17. Fluorescent spectra of L^1 and complex **1** (a) and L^2 and complex **3** (b) in the solid state at room temperature.

Acknowledgments

We thank the National Natural Science Foundation of China (50532030, 50325311, and 50335050), the Doctoral Program Foundation of the Ministry of Education of China, the Education Committee of Anhui Province (2006KJ032A and 2006KJ135B), the People with Ability Foundation of Anhui Province (2002Z021), the Team for Scientific Innovation Foundation of Anhui Province (2006KJ007TD), the Key Laboratory of Opto-Electronic Information Acquisition and Manipulation (Anhui University), and the

Ministry of Education, People with Ability Foundation of Anhui University for financial support.

[1] B. Moulton, M. J. Zaworotko, *Chem. Rev.* **2001**, *101*, 1629.

[2] a) M. J. Zaworotko, *Chem. Commun.* **2001**, 1; b) S. R. Batten, R. Robson, *Angew. Chem. Int. Ed.* **1998**, *37*, 1460; c) S. Kitagawa, M. Kondo, *Bull. Chem. Soc. Jpn.* **1998**, *71*, 1739; d) G. R. Desiraju, *Angew. Chem. Int. Ed. Engl.* **1995**, *34*, 2311.

[3] a) C. Janiak, *Angew. Chem. Int. Ed. Engl.* **1997**, *36*, 1431; b) C. Janiak, *Dalton Trans.* **2003**, 2781; c) O. M. Yaghi, H. Li, C. Davis, D. Richardson, T. L. Groy, *Acc. Chem. Res.* **1998**, *31*, 474.

[4] a) M. Eddaoudi, H. Li, O. M. Yaghi, *J. Am. Chem. Soc.* **2000**, *122*, 1391; b) H. Li, M. Eddaoudi, T. L. Groy, O. M. Yaghi, *J. Am. Chem. Soc.* **1998**, *120*, 8571; c) T. M. Reineke, M. Eddaoudi, M. Fehr, D. Kelley, O. M. Yaghi, *J. Am. Chem. Soc.* **1999**, *121*, 1651; d) N. L. Rosi, J. Eckert, M. Eddaoudi, D. T. Vodak, J. Kim, M. O'keeffe, O. M. Yaghi, *Science* **2003**, *300*, 1127; e) R. Kitaura, K. Seki, G. Akiyama, S. Kitagawa, *Angew. Chem. Int. Ed.* **2003**, *42*, 428; f) M. L. Tong, J. X. Shi, X. M. Chen, *New J. Chem.* **2002**, *26*, 814; g) W. B. Lin, L. Ma, O. R. Evans, *Chem. Commun.* **2000**, 2263; h) G. S. Matouzenko, G. Molnar, N. Brefuel, M. Perrin, A. Bousseksou, S. A. Borshch, *Chem. Mater.* **2003**, *15*, 550; i) V. Niel, A. L. Thompson, M. C. Muñoz, A. Galet, A. E. Goeta, J. A. Real, *Angew. Chem. Int. Ed.* **2003**, *42*, 3760; j) O. R. Evans, H. L. Ngo, W. Lin, *J. Am. Chem. Soc.* **2001**, *123*, 10395; k) J. S. Seo, D. Whang, H. Lee, S. I. Jun, J. Oh, Y. J. Jeon, K. Kim, *Nature* **2000**, *404*, 982; l) M. Fujita, Y. J. Kwon, S. Washizu, K. Ogura, *J. Am. Chem. Soc.* **1994**, *116*, 1151.

[5] a) O. M. Yaghi, G. M. Li, H. Li, *Nature* **1995**, *378*, 703; b) O. M. Yaghi, H. Li, T. L. Groy, *J. Am. Chem. Soc.* **1996**, *118*, 9096.

[6] a) C. Kirchner, B. Krebs, *Inorg. Chem.* **1987**, *26*, 3569; b) C. A. Hester, H. L. Collier, R. G. Baughman, *Polyhedron* **1996**, *15*, 4255; c) A. S. Abushamleh, H. A. Goodwin, *Aust. J. Chem.* **1979**, *32*, 513; d) U. Sakaguchi, A. W. Addison, *J. Chem. Soc., Dalton Trans.* **1979**, 600; e) A. Bendini, F. Mani, *Inorg. Chim. Acta* **1988**, *154*, 215; f) S. Fortin, A. L. Beauchamp, *Inorg. Chem.* **2000**, *39*, 4886; g) M. A. M. Lorente, F. Dahan, V. Petrouleas, A. Boussedsou, J.-P. Tuchagues, *Inorg. Chem.* **1995**, *34*, 5346; h) I. G. Dance, A. S. Abushamleh, H. A. Goodwin, *Inorg. Chim. Acta* **1980**, *43*, 217; i) A. D. Mighell, C. W. Reimann, F. A. Maucer, *Acta Crystallogr., Sect. B* **1969**, *25*, 60; j) J. Cancela, M. J. G. Garmendia, M. Quriós, *Inorg. Chim. Acta* **2001**, *313*, 156; k) R. Sang, M. Zhu, P. Yang, *Acta Crystallogr., Sect. E* **2002**, *58*, 172; l) B. H. Ye, F. Xue, G. Q. Xue, L. N. Ji, T. C. W. Mak, *Polyhedron* **1999**, *18*, 1785; m) C. A. Hester, R. G. Baughman, H. L. Collier, *Polyhedron* **1997**, *16*, 2893.

[7] a) S. W. Kaiser, R. B. Saillant, W. M. Butler, P. G. Rasmussen, *Inorg. Chem.* **1976**, *15*, 2681; b) S. W. Kaiser, R. B. Saillant, P. G. Rasmussen, *J. Am. Chem. Soc.* **1975**, *97*, 425; c) S. W. Kaiser, R. B. Saillant, W. M. Butler, P. G. Rasmussen, *Inorg. Chem.* **1976**, *15*, 2688; d) M. S. Haddad, D. N. Hendrickson, *Inorg. Chem.* **1978**, *17*, 2622; e) R. Usón, J. Gimeno, J. Forniés, F. Martínez, *Inorg. Chim. Acta* **1981**, *50*, 173; f) A. Maiboroda, G. Rheinwald, H. Lang, *Inorg. Chem. Commun.* **2001**, *4*, 381; g) P. Majumdar, S. M. Peng, S. Goswami, *J. Chem. Soc., Dalton Trans.* **1998**, 1569; h) R. Usón, L. A. Oro, J. Gimeno, M. A. Ciriano, J. A. Cabeza, *J. Chem. Soc., Dalton Trans.* **1983**, 323; i) A. P. Sadimenko, S. S. Basson, *Coord. Chem. Rev.* **1996**, *147*, 247.

[8] a) J. S. Casas, A. Castiñeiras, Y. Parajó, M. L. P. Parallé, A. Sánchez, A. S. González, J. Sordo, *Polyhedron* **2003**, *22*, 1113; b) A. S. Gonzalez, J. S. Casas, J. Sordo, U. Russo, M. I. Lareo, B. J. Regueiro, *J. Inorg. Biochem.* **1990**, *39*, 227; c) C. Lopez, A. Sanchez-Gonzalez, M. E. Garcia, J. S. Casas, J. Sordo, R. Graziani, U. Casellato, *J. Organomet. Chem.* **1992**, *434*, 261; d) B. J. Holliday, C. A. Mirkin, *Angew. Chem. Int. Ed.* **2001**, *40*, 2022; e) J. D. Watson, F. H. C. Crick, *Nature* **1953**, *171*, 737; f) P. A. Zoo, J. S. Casas, M. D. Couse, E. Freijanes, A. Furlani, V. Scarcial, J. Sordo, U. Russo, M. Varela, *Appl. Organomet. Chem.* **1997**, *11*, 963.

[9] a) M. Tadokoro, K. Isobe, H. Uekusa, Y. Ohashi, J. Toyoda, K. Tashiro, K. Nakasuji, *Angew. Chem. Int. Ed.* **1999**, *38*, 95; b) M. Tadokoro, H. Kanno, T. Kitajima, H. Shimada-Umemoto, N. Nakanishi, K. Isobe, K. Nakasuji, *Proc. Natl. Acad. Sci. USA* **2002**, *99*, 4950; c) M. Tadokoro, T. Shiomi, K. Isobe, K. Nakasuji, *Inorg. Chem.* **2001**, *40*, 5476; d) M. Tadokoro, K. Nakasuji, *Coord. Chem. Rev.* **2000**, *198*, 205; e) R. Atencio, M. Chacón, T. González, A. Briceño, G. Agrifoglio, A. Sierraalta, *Dalton Trans.* **2004**, 505; f) W. E. Allen, C. J. Fowler, V. M. Lynch, J. L. Sessler, *Chem. Eur. J.* **2001**, *7*, 721; g) L. Öhrström, K. Larsson, S. Borg, S. T. Norberg, *Chem. Eur. J.* **2001**, *7*, 4805; h) C. Pettinari, R. Pettinari, *Coord. Chem. Rev.* **2005**, *249*, 525.

[10] a) C. Y. Su, Y. P. Cai, C. L. Chen, M. D. Smith, W. Kaim, H. C. zur Loye, *J. Am. Chem. Soc.* **2003**, *125*, 8595; b) J. Fan, B. Sui, T. A. Okamura, W. Y. Sun, W. X. Tang, N. Ueyama, *J. Chem. Soc., Dalton Trans.* **2002**, 3868; c) H. K. Liu, W. Y. Sun, W. X. Tang, H. Y. Tan, H. X. Zhang, Y. X. Tong, X. L. Yu, B. Sh. Kang, *J. Chem. Soc., Dalton Trans.* **2002**, 3886; d) J. Fan, L. Gan, H. Kawaguchi, W. Y. Sun, K. B. Yu, W. X. Tang, *Chem. Eur. J.* **2003**, *9*, 3965; e) S. Y. Wan, Y. Z. Li, T. A. Okamura, J. Fan, W. Y. Sun, N. Ueyama, *Eur. J. Inorg. Chem.* **2003**, 3783; f) S. Y. Wan, J. Fan, T. A. Okamura, H. F. Zhu, X. M. Ouyang, W. Y. Sun, N. Ueyama, *Chem. Commun.* **2002**, 2520.

[11] a) H. P. Zhou, J. Zh. Zhang, D. M. Li, Y. M. Zhu, Zh. J. Hu, J. Y. Wu, Y. Xie, M. H. Jiang, X. T. Tao, Y. P. Tian, *J. Mol. Struct.* **2005**, *743*, 93; b) H. P. Zhou, Y. P. Tian, J. Y. Wu, J. Zh. Zhang, D. M. Li, Y. M. Zhu, Zh. J. Hu, X. T. Tao, M. H. Jiang, Y. Xie, *Eur. J. Inorg. Chem.* **2005**, 4976.

[12] F. D. Hager, *Org. Synthesis*, Col. Vol. 1, 2nd Ed. **1948**, 544.

[13] C. J. Horn, A. J. Blake, N. R. Champness, A. Garau, V. Lippolis, C. Wilson, M. Schröder, *Chem. Commun.* **2003**, 312.

[14] G. Barberà, C. Viñas, F. Teixidor, G. M. Rosair, A. J. Welch, *J. Chem. Soc., Dalton Trans.* **2002**, 3647.

[15] L. Y. Kong, Zh. H. Zhang, T. A. Okamura, M. J. Fei, W. Y. Sun, N. Ueyama, *Chem. Lett.* **2004**, *33*, 1572.

[16] a) F. H. Allen, C. M. Bird, R. S. Rowland, P. R. Raithby, *Acta Crystallogr., Sect. Sect. B* **1997**, *53*, 696; b) A. D. Bond, W. Jones, *J. Chem. Soc., Dalton Trans.* **2001**, 3045.

[17] H. F. Zhu, L. Y. Kong, T. A. Okamura, J. Fan, W. Y. Sun, N. Ueyama, *Eur. J. Inorg. Chem.* **2004**, 1465.

[18] Y. Zheng, M. Du, J. R. Li, R. H. Zhang, X. H. Bu, *Dalton Trans.* **2003**, 1509.

[19] Y. B. Dong, M. D. Smith, H. C. zur Loye, *Inorg. Chem.* **2000**, *39*, 4927.

[20] G. R. Desiraju, *Acc. Chem. Res.* **1996**, *29*, 441.

[21] I. Unamuno, J. M. Gutiérrez-Zorrilla, A. Luque, P. Román, L. Lezama, R. Calvo, T. Rojo, *Inorg. Chem.* **1998**, *37*, 6452.

[22] C. V. K. Sharma, R. D. Rogers, *Cryst. Eng.* **1998**, *1*, 19.

[23] a) K. N. Power, T. L. Hennigar, M. J. Zaworotko, *New J. Chem.* **1998**, *22*, 177; b) O. S. Jung, S. H. Park, K. M. Kim, H. G. Jang, *Inorg. Chem.* **1998**, *37*, 5781; c) P. Losier, M. J. Zaworotko, *Angew. Chem. Int. Ed. Engl.* **1996**, *35*, 2779; d) H. Gudbjartson, K. Biradha, K. M. Poirier, M. J. Zaworotko, *J. Am. Chem. Soc.* **1999**, *121*, 2599; e) L. Carlucci, G. Ciani, D. M. Proserpio, *J. Chem. Soc., Dalton Trans.* **1999**, 1799; f) Y. B. Dong, R. C. Layland, N. G. Pschirer, M. D. Smith, U. H. F. Bunz, H. C. zur Loye, *Chem. Mater.* **1999**, *11*, 1413.

[24] a) M. Du, X. H. Bu, Z. Huang, S. T. Chen, Y. M. Guo, C. Diaz, J. Ribas, *Inorg. Chem.* **2003**, *42*, 552; b) X. H. Bu, W. Chen, S. T. Lu, R. H. Zhang, D. Z. Liao, W. M. Bu, M. Shionoya, F. Brisse, J. Ribas, *Angew. Chem. Int. Ed.* **2001**, *40*, 3201; c) F. A. A. Paz, Y. Z. Khimyak, A. D. Bond, J. Rocha, J. Klinowski, *Eur. J. Inorg. Chem.* **2002**, 2823; d) Y. B. Dong, M. D. Smith, R. C. Layland, H. C. zur Loye, *Inorg. Chem.* **1999**, *38*, 5027.

[25] a) L. Y. Zhang, G. F. Liu, S. L. Zheng, B. H. Ye, X. M. Zhang, X. M. Chen, *Eur. J. Inorg. Chem.* **2003**, 2965; b) J. H. Luo,

M. C. Hong, R. H. Wang, R. Cao, L. Han, Z. Z. Lin, *Eur. J. Inorg. Chem.* **2003**, 2705; c) B. C. Tzeng, H. T. Yeh, *Z. Naturforsch., Teil B* **2004**, *59*, 1320; d) B. C. Tzeng, B. S. Chen, H. T. Yeh, G. H. Lee, S. M. Peng, *New J. Chem.* **2006**, *30*, 1087.

[26] G. M. Sheldrick, *SHELXL-97, Program for Crystal Structure Refinement*, University of Göttingen, Germany, **1997**.

Received: September 22, 2006
Published Online: March 20, 2007

